Proc. of the International Conference on Mechanochemistry and Mechanical Alloying, Kraków, Poland, June 22–26, 2014

Electric Conductivity of $(Bi_{1-x}La_xFeO_3)_{0.5}(PbTiO_3)_{0.5}$ Ceramics Obtained from Mechanosynthesized Nanopowders

E. Markiewicz[a,*], B. Hilczer[a], M. Balcerzak[b] and M. Jurczyk[b]

[a]Institute of Molecular Physics, Polish Academy of Sciences, M. Smoluchowskiego 17, 60-179 Poznań, Poland

[b]Institute of Materials Science and Engineering, Poznań University of Technology, pl. M. Skłodowskiej-Curie 5, 60-965 Poznań, Poland

Electric conductivity of $(Bi_{1-x}La_xFeO_3)_{0.5}(PbTiO_3)_{0.5}$ ceramics obtained from nanopowders synthesized by high-energy milling from respective oxides was studied in the frequency range 10 mHz ÷1 GHz. At room temperatures the low-frequency conductivity was found to be dominated by the contribution from poor-conducting grain boundaries, whereas the contribution in the range 1 kHz ÷ 1 MHz, due to the grain interior, was related by us to the small polaron hopping. Moreover, the electron exchange between ferric and ferrous ions activated at higher frequencies was found to be added to the conductivity above ≈ 1 MHz.

DOI: 10.12693/APhysPolA.126.971

PACS: 81.07.Bc, 81.07.Wx, 81.20.Ev, 75.85.+t, 81.40.Rs

1. Introduction

Bismuth ferrite $BiFeO_3$ (BFO) is one of the most extensively studied multiferroic materials due to its antiferromagnetic and ferroelectric order at room temperature. The application of BFO is, however, limited because of weak magnetoelectric coupling characteristic of multiferroics with large difference between the ferroelectric-paraelectric transition temperatures ($T_C = 1100$ K) and the Néel temperature ($T_N = 640$ K) [1]. The synthesis of BFO-based multiferroics with a strong coupling between spontaneous polarization and magnetization is still challenging for possible applications in transducers, resistive switching elements, information storage, and spintronics [2–6]. One of the methods used is to form solid solutions with ABO_3 perovskites and $PbTiO_3$ (PT) has been considered as the most promising candidate [7]. Interesting results were reported by Zhu et al. who established both the structural and the magnetic phase diagram of (1-y)$BiFeO_3$-$y$$PbTiO_3$ system [8]. The authors reported rhombohedral structure for $y \leq 0.20$, orthorhombic symmetry for solutions with $0.20 \leq y \leq 0.28$ and tetragonal phase for $y \geq 0.31$. Moreover, they pointed out that the compositions with $BiFeO_3$:$PbTiO_3$ ratio around 50:50 favors a formation of chemically ordered microregions (with superlattices of Fe^{3+} and Ti^{4+}). La^{3+} doping was proposed to improve the magnetoelectric effect in $BiFeO_3$ by Pająk, Połomska and Kaczmarek [9, 10] and by Sosnowska et al. [11]. The doping has been used to the (1-y)$BiFeO_3$-$y$$PbTiO_3$ system a decade later [12–18].

The properties of La^{3+} doped $(BiFeO_3)_{0.5}(PbTiO_3)_{0.5}$ with lanthanum content $0 \leq x \leq 0.5$ synthesized by solid-state reaction technique were studied repeatedly [14, 16–19] and the resulting $T-x$ phase diagram points to a tetragonal symmetry with $P4mm$ space group for low La-content, whereas rhombohedral symmetry with $R3c$ space group was ascribed to the solution with $x = 0.5$. As the compounds of BFO with $PbTiO_3$ exhibit structural change from rhombohedral to tetragonal structure [8] and La^{3+} doping may turn the structure again to the rhombohedral symmetry [1, 11], we prepared $(Bi_{1-x}La_xFeO_3)_{0.5}(PbTiO_3)_{0.5}$ solid solutions (BLFO–PT) with various La contents. The BLFO–PT nanopowders were prepared by mechanochemical synthesis from respective oxides since we considered the method, in the case of compounds containing high volatile elements like Pb and Bi, as superior in comparison with the solid-state synthesis [20–22].

The results of the Raman spectroscopy studies of the obtained nanopowders pointed to a change in the crystallographic structure of the BLFO–PT solutions with La-content between $x = 0.16$ and $x = 0.20$ [23]. Our dielectric response studies revealed also relaxor-like behavior below 300 K in ceramics prepared from the mechanosynthesized nanopowders due to structural disorder, an anomaly at ≈ 400 K related to oxygen vacancies and only for solution with $x = 0.50$ the Curie point anomaly at ≈ 500 K was observed [24]. Moreover, a coexistence of ferromagnetic clusters and antiferromagnetic order as well as spin glass behavior have been reported for the samples. From the application point of view, one of the important properties is the conductivity that should be properly matched to the electric impedance of the sensor or actuator circuits. Here we present the results of electric conductivity studies in wide frequency range from 10^{-2} Hz to 1 GHz of BLFO–PT solid solution. The work was also aimed at finding the relationship between the La^{3+} content and the conductivity. The results of the conductivity measurements allowed to determine the structural transition at appropriate La^{3+} content and were compared to that of the Raman studies.

*corresponding author; e-mail: ewamar@ifmpan.poznan.pl

2. Experimental

The synthesis of BLFO–PT samples with various La content $x = 0$, 0.10, 0.16, 0.18, 0.20, 0,22, 0.25, 0.28, 0.30, 0.32, 0.35, and 0.50 was carried out in a SPEX 8000 Mixer Mill for 48 h at room temperature in air. The milling time was optimized using XRD patterns for various times. Figure 1 shows an example of XRD patterns (X'Pert-PANalytical diffractometer, Cu K_α radiation) of the mixture of Bi_2O_3, Fe_2O_3, PbO and TiO_2 powders after various times of milling. One can observe that after 48 h of milling diffraction peaks corresponding to the perovskite tetragonal structure of BLFO–PT appear and remain unchanged with elongation of the time of milling. The starting oxides Bi_2O_3 (99.975% Alfa Aesar), La_2O_3 (99.99% Aldrich), Fe_2O_3 (99.9% Aldrich), PbO (99.9% Aldrich) and TiO_2 ($\geq$ 99% Aldrich) were weighted in stoichiometric ratios and the weight ratio of the stainless steel balls to the oxides was 2:1. The as-milled powders were heat treated at 973 K for 0.5 h in air. The average crystallite sizes of $(Bi_{1-x}La_xFeO_3)_{0.5}(PbTiO_3)_{0.5}$ samples estimated from half-width of the most intensive (110) peak (Scherrer eq., Panalytical High Score program) amounted to 15, 19, 26, 27, and 28 nm for $x = 0.0$, 0.1, 0.2, 0.3 and 0.5, respectively.

The samples in form of pellets $\approx$ 1 mm thick and 8 mm in diameter were obtained after pressing the nanopowder under 800 MPa and for electric measurements the samples were covered with gold sputtered electrodes. The ac conductivity of the samples was measured using an Alpha-A High Performance Frequency Analyzer (Novocontrol GmbH) in the frequency range 10^{-2} Hz $\div$ 1 MHz and temperatures from 125 K to 525 K and at room temperature using a E4991A RF Impedance/Material Analyzer Agilent for higher frequencies up to 1 GHz.

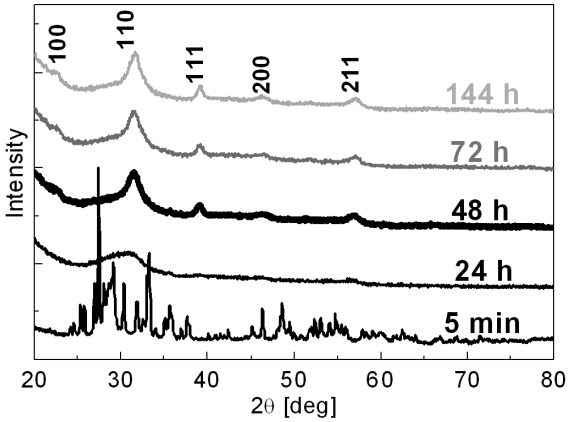

Fig. 1. XRD patterns of Bi_2O_3, Fe_2O_3, PbO and TiO_2 mixture after various times of milling.

3. Results and discussion

Figure 2 shows temperature variation of the conductivity σ' at various frequencies for $(Bi_{1-x}La_xFeO_3)_{0.5}(PbTiO_3)_{0.5}$ ceramic samples with various La content.

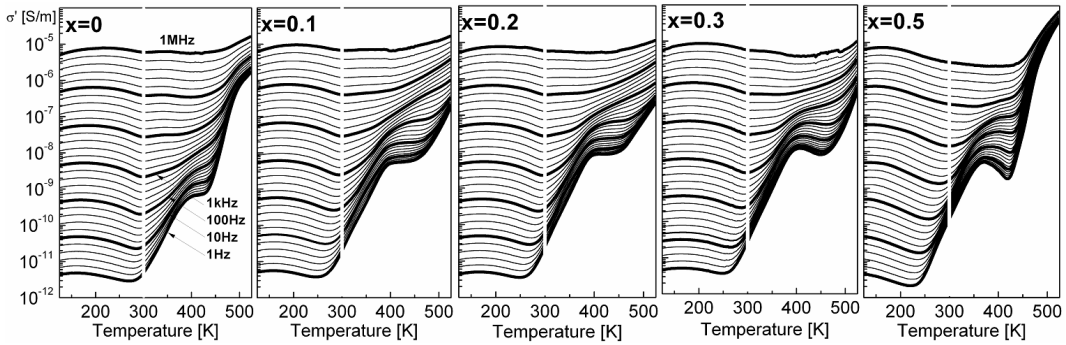

Fig. 2. Temperature variation of electric conductivity for $(Bi_{1-x}La_xFeO_3)_{0.5}(PbTiO_3)_{0.5}$ ceramics at frequencies of 1 Hz, 1.58 Hz, 2.51 Hz, 3.98 Hz, 6.31 Hz, 10 Hz, 15.8 Hz, 25.1 Hz... 100 kHz, 158 kHz, 251 kHz, 398 kHz, 631 kHz, 1 MHz.

As indicated by the white vertical line in Fig. 2, La doping affects the low-frequency dispersion of σ' in the vicinity of room temperature. Figure 3 shows frequency dependences of the conductivity and dielectric permittivity for samples in the La-content range where the changes in the Raman spectra have been observed [23]. It should be noted that the conductivity σ' measured at a given frequency f and temperature T contains a frequency independent contribution $\sigma'_{\rm dc}$ and a contribution $\sigma'_{\rm ac}$ which depends on the frequency f: $\sigma'(T,f) = \sigma'_{\rm dc}(T) + \sigma'_{\rm ac}(T,f)$. The first term is related to the drift mobility of the charge carriers, whereas the heterogeneity of the sample determines the $\sigma'_{\rm ac}(T,f)$ behavior [25–27]. The heterogeneity of BFLO–PT ceramics is rather complex and we have to consider that as consisting of highly-conducting grains separated by grain boundaries with high electric resistivity [27].

Defects as oxygen vacancies apparent in the perovskite lattice ($\square O^{2-} + h \Leftrightarrow \square O^{-}$ and $\square O^{-} + h \Leftrightarrow \square O$) as well as defects created by La^{3+} substitution at the place of divalent A ions ($La^{3+} + e \Leftrightarrow \square A^{2+}$), Fe^{3+} substitution at the tetravalent B ion ($Fe^{3+} + h \Leftrightarrow \square B^{4+}$) are piled up at the grain boundaries [28]. Moreover, in our case we have to take into account various valence of Fe ions ($Fe^{3+} + h \Leftrightarrow Fe^{4+}$) [29]. In the text above, vacancy is denoted as empty square, hole as h and electron as e.

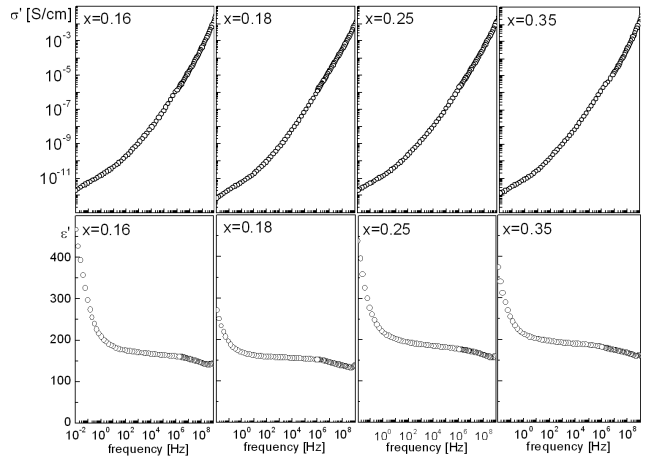

Fig. 3. Frequency dependences of the conductivity σ' and dielectric losses ($\tan\delta$) of $(Bi_{1-x}La_xFeO_3)_{0.5}(PbTiO_3)_{0.5}$ ceramic samples with various x at room temperature.

The motion of the charges in external electric field E results in a space charge polarization accumulated at the grain boundaries. When the frequency f of E increases the charge hopping between the ions/vacancies of different valence cannot follow the ac field and the dielectric permittivity ε' decreases. The grain boundary effect is predominant at low frequencies [27] and for BLFO–PT ceramics one can observe the contribution from 10^{-2} Hz to ≈ 1 kHz at room temperature (Fig. 3). At higher frequencies the conductivity is mainly due to the interior of the grains with a structural disorder and the $\sigma'_{\rm ac}$ (f) values in the frequency range from ≈ 1 kHz to ≈ 1 MHz at room temperature are nearly proportional to the frequency f. It should be observed that the energy levels of electrons and holes in the material are localized on specific atoms/vacancies which can appear in different valence states, therefore we would like to consider thermally activated motion of electrons and holes to adjacent sites as small polaron hopping [28, 29]. An increase in the conductivity at higher frequencies may be related to a contribution of another process for instance $Fe^{3+} + e \rightarrow Fe^{2+}$ electron hopping enhanced by the increase in the frequency of applied electric field.

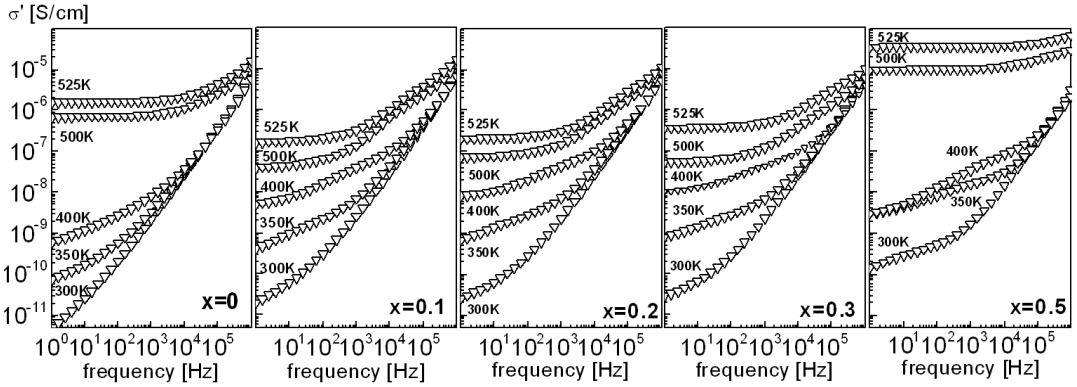

Fig. 4. ac conductivity of $(Bi_{1-x}La_xFeO_3)_{0.5}$ $(PbTiO_3)_{0.5}$ ceramics at various temperatures.

Frequency dependences of the conductivity at various temperatures are shown in Fig. 4. One can observe that above ≈ 400 K the conductivity attains a plateau at low frequencies, which points to the fact that the space charge polarization is effective at high temperatures and low frequencies. Temperature variation of the dc conductivity $\sigma'(1\text{ Hz})$ of $(Bi_{1-x}La_xFeO_3)_{0.5}(PbTiO_3)_{0.5}$ above 450 K can be described by the Arrhenius law with activation energies 1.23, 1.18, 0.98, 1.47 and 1.41 eV for ceramics with $x = 0$, 0.1, 0.2, 0.3 and 0.5, respectively.

The low-frequency ac conductivity of $(Bi_{1-x}La_xFeO_3)_{0.5}(PbTiO_3)_{0.5}$ ceramics was found to be dependent on the lanthanum content as shown in Fig. 5a with minimum $\sigma'_{\rm ac}$ values at the concentration $x = 0.18$.

Similar dependence on La content was found also in the dielectric losses measured at low frequencies for BFLO–PT ceramic samples. Dielectric loss factor ($\tan\delta$), a measure of electric energy dissipated in the dielectric system, shows minimum for La^{3+} ion content $x = 0.18$ as shown in Fig. 5b. In the low-frequency region the dielectric losses are related to space charge polarization piled up at the low-conducting grain boundaries.

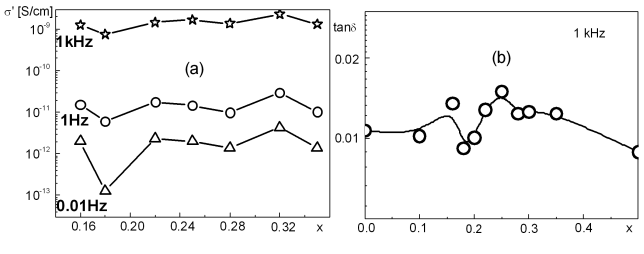

Fig. 5. Room temperature electric conductivity σ' at frequencies of 0.01 Hz, 1 Hz and 1 kHz (a) and dielectric losses at 1 kHz for $(Bi_{1-x}La_xFeO_3)_{0.5}(PbTiO_3)_{0.5}$ ceramic samples with various x.

4. Conclusions

$(Bi_{1-x}La_xFeO_3)_{0.5}(PbTiO_3)_{0.5}$ solid solutions obtained by solid state reaction have been studied by

many authors at the aim to improve the magnetoelectric coupling in $BiFeO_3$ based compounds. To provide a proper stoichiometry in the compounds containing volatile elements as Pb and Bi we synthesized $(Bi_{1x}La_xFeO_3)_{0.5}(PbTiO_3)_{0.5}$ nanopowders by high-energy milling of respective oxides and studied ac electric conductivity of the ceramics prepared from the nanopowders in frequency range 10 mHz ÷ 1 GHz. The conductivity was found to be determined by the heterogeneity of the ceramics consisting of poor-conducting grain boundaries and the grain interiors with substitutional disorder (La^{3+} cations in the A-sites and Fe^{3+} in the B-sites of the perovskite lattice). At room temperatures the conductivity at low frequencies (10 mHz ÷ 1 kHz) was found to be dominated by the contribution from the grain boundaries, whereas the at higher frequencies the contribution from the grain interior was found to be the most important. The conductivity in the frequency range 1 kHz ÷ 1 MHz was related by us to small polaron hopping. The effect of La^{3+} doping is the most apparent one as an increase in the low-frequency dispersion in the conductivity. In the vicinity of room temperature the conductivity at 1 Hz increases by about of two orders of magnitude for BLFO–PT ceramics with the highest contents of La^{3+} in comparison with that of BLFO–PT samples. Moreover, the substitutional disorder due to the substitution of La^{3+} ions contributes to the high-frequency conductivity in BLFO-PT ceramics.

The low-frequency electric conductivity, as well as the low-frequency dielectric losses of $(Bi_{1-x}La_xFeO_3)_{0.5}(PbTiO_3)_{0.5}$ ceramics were found to exhibit minimum at $x = 0.18$ (Figs. 4 and 5) i.e. in the vicinity of the La^{3+} concentrations at which we have observed considerable changes in the Raman spectra. The results allow us to assume a morphotropic phase boundary in the vicinity of $x = 0.18$, or even to expect a coexistence of the tetragonal and rhombohedral phases in the La concentration range $\approx 0.16 \leq x \leq \approx 0.32$. It should be observed that the material exhibits also ferroelastic properties and structural changes in the interior of the grains modify also the properties of the grain boundaries.

Acknowledgments

The work was done within the frame of COST Action MP 0904 "Single- and multiphase ferroics and multiferroics with restricted geometries (SIMUFER)".

References

[1] G. Catalan, J.F. Scott, *Adv. Mater.* **21**, 2463 (2009).

[2] F. Yang, M.H. Tang, Z. Ye, Y.C. Zhou, X.J. Zheng, J.X. Tang, J.J. Zhang, J. He, *J. Appl. Phys.* **102**, 044504 (2007).

[3] M. Bibes, A. Barthelemy, *Nature Mater.* **7**, 425 (2008).

[4] H. Béa, M. Gajek, M. Bibes, A. Barthélémy, *J. Phys. Condens. Matter* **20**, 434221 (2008).

[5] Y.-H. Chu, L.W. Martin, M.B. Holcomb, M. Gajek, S.-J. Han, Q. He, N. Balke, C.-H. Yang, D. Lee, W. Hu, Q. Zhan, P.-L. Yang, A.F. Rodríguez, A. Scholl, S.X. Wang, R. Ramesh, *Nature Mater.* **7**, 478 (2008).

[6] P. Rovillain, R. de Sousa, Y. Gallais, A. Sacuto, M.A. Méasson, D. Colson, A. Forget, M. Bibes, A. Barthélémy, M. Cazayous, *Nature Mater.* **9**, 975 (2010).

[7] Y.N. Venevtsev, G.S. Zhdanov, S.P. Solov'ev, E.V. Bezus, V.V. Ivanova, S.A. Fedulov, A.G. Kapyshev, *Sov. Phys. Crystallogr.* **5**, 594 (1960).

[8] W.M. Zhu, H.Y. Guo, Z.G. Ye, *Phys. Rev. B* **78**, 014401-1-9 (2008).

[9] M. Połomska, W. Kaczmarek, Z. Pająk, *Phys. Status Solidi A* **23**, 567 (1974).

[10] W. Kaczmarek, Z. Pająk, M. Połomska, *Solid State Commun.* **17**, 807 (1975).

[11] I. Sosnowska, R. Przeniosło, P. Fischer, V.A. Murashov, *J. Magn. Magn. Mater.* **160**, 384 (1996).

[12] J. Cheng, S. Yu, J. Chen, Z. Meng, L.E. Cross, *Appl. Phys. Lett.* **89**, 122911 (2006).

[13] Z.A. Li, H.X. Yang, H.F. Tian, J.Q. Lia, J. Cheng, J. Chen, *Appl. Phys. Lett.* **90**, 182904 (2007).

[14] A. Singh, A. Gupta, R. Chatterjee, *Appl. Phys. Lett.* **93**, 022902 (2008).

[15] T. Leist, T. Granzow, W. Jo, J. Rödel, *J. Appl. Phys.* **108**, 014103 (2010).

[16] K.K. Mishra, V. Sivasubramanian, R.M. Sarguna, T.R. Ravindran, A.K. Arora, *J. Solid State Chem.* **184**, 2381 (2011).

[17] K.K. Mishra, A.T. Satya, A. Bharathi, V. Sivasubramanian, V.R.K. Murthy, A.K. Arora, *J. Appl. Phys.* **110**, 123529 (2011).

[18] K.K. Mishra, R.M. Sarguna, S. Khan, A.K. Arora, *AIP Adv.* **1**, 032126 (2011).

[19] A. Singh, R. Chatterjee, S.K. Mishra, P.S.R. Krishna, S.L. Chaplot, *J. Appl. Phys.* **111**, 014113 (2012).

[20] L.B. Kong, T.S. Zhang, J. Ma, F. Boey, *Prog. Mater. Sci.* **53**, 207 (2008).

[21] I. Szafraniak-Wiza, W. Bednarski, S. Waplak, B. Hilczer, A. Pietraszko, L. Kępiński, *J. Nanosci. Nanotechnol.* **9**, 3246 (2009).

[22] E. Markiewicz, B. Hilczer, M. Błaszyk, A. Pietraszko, E. Talik, *J. Electroceram.* **27**, 154 (2011).

[23] M. Połomska, B. Hilczer, J. Wolak, A. Pietraszko, M. Balcerzak, M. Jurczyk, J. Jakubowicz, *Phase Transit.*, published online 2014.

[24] E. Markiewicz, B. Andrzejewski, B. Hilczer, M. Balcerzak, A. Pietraszko, M. Jurczyk, *J. Electroceram.*, submitted for publication.

[25] J.C. Maxwell, *Electric and Magnetism*, Vol. 2, Oxford University Press, New York 1973, p. 828.

[26] K.W. Wagner, *Ann. Phys.* **40**, 817 (1913).

[27] C.G. Koops, *Phys. Rev.* **83**, 121 (1951).

[28] M. Maglione, arXiv:1006.3719.

[29] M. Idrees, M. Nadeem, M. Atif, M. Siddique, M. Mehmood, M.M. Hassan, *Acta Mater.* **59**, 1338 (2011).